Title: The NPH3-domain protein NRL5 is a plant specific type of GTPase essential for drought resistance

Authors: Neha Upadhyay-Tiwari[1], Xin-Jie Huang[1], Yi-Chen Lee[1]†, Shashi Kant Singh[1]†, Chuan-Chi Hsu[1], Shih-Shan Huang[1], Paul E. Verslues[1]*

Affiliations:

[1]Institute of Plant and Microbial Biology, Academia Sinica; Taipei, 11529, Taiwan

*Corresponding author. Email: paulv@gate.sinica.edu.tw

†These authors contributed equally to this work.

Abstract: Intracellular trafficking is essential to maintain the plasma membrane-cell wall interface, a site where environmental stimuli such as limited water availability can be perceived. However, the identity of plant trafficking regulators, and their relationship to drought resistance, is unclear. An amino acid substitution in the Non-Phototrophic Hypocotyl3 (NPH3) domain of NPH3/RPT2-Like5 (NRL5)/Naked Pins in Yucca8 (NPY8) causes extreme drought sensitivity due to mis-regulated proline metabolism. This NPH3-domain mutation inhibits NRL5 GTPase activity, disrupts interaction with RAB small GTPases and the SNARE proteins VAMP721/722, and diminishes NRL5 polar localization. Our finding that the NPH3 domain is plant specific type of GTPase participating in intracellular trafficking provides a basis to understand NPH3-domain function in diverse processes including abiotic stress resistance, hormone signaling and maintenance of cellular polarity.

One-Sentence Summary: GTP association and trafficking interaction of the NPH3 domain is essential for NRL5 function in drought resistance.

Main Text:

Even moderate severity drought stress (moderate reduction of water potential, ψ_w) leads to reprogramming of cellular processes to retain water while also preparing for more severe water limitation. Thus, plants can detect and initiate signaling in response to small shifts in water status. How this occurs is not known but may include sensing and signaling events at the plasma membrane-cell wall interface (*1-3*). Intracellular trafficking that maintains these cellular locations may also be hypothesized to influence drought sensitivity. However, trafficking regulation in plants, and its relationship to drought response, is unclear and likely to involve both proteins that are functionally conserved compared to their metazoan counterparts as well as plant-specific proteins yet to be identified.

Many plants accumulate free proline during drought. Proline serves as a protective solute to increase cellular osmolarity and precise regulation of the proline cycle of synthesis and catabolism balances redox status (*4, 5*). Proline Dehydrogenase (ProDH) catalyzes the first step of mitochondrial proline catabolism and allows proline to serve as alternative respiratory substrate (*6, 7*). *ProDH1* is induced by exogenous proline during and drought recovery (re-watering) when high levels of proline need to be catabolized (*5-7*). However, during drought stress *ProDH1* is down regulated despite high levels of proline accumulation. In this case, drought-related signaling overrides the metabolic signal of high proline (*8, 9*). In contrast, during the hypersensitive response to pathogen infection, *ProDH* up-regulation, along with increased proline synthesis, leads to high levels of mitochondrial ROS and Δ^1-pyrroline-5-carboxylate (P5C), the metabolic intermediate of proline catabolism and synthesis, which promote cell death (*10, 11*). These seemingly opposing purposes of proline metabolism, to sustain cellular activity on the one hand but induce cell death on the other, have been observed in both plants and in metazoans, where ProDH activity can be a determinant of cancer progression (*2, 12, 13*). There is some evidence that plasma membrane-

derived signals are required for stress-induced proline accumulation (*14, 15*); however, the mechanisms that regulate and balance the seemingly opposing roles of proline metabolism remain unknown in any biological system.

To understand this intersection of drought and metabolic signaling, we conducted a forward genetic screen using a *ProDH1 promoter:luciferase* (*ProDH1$_{pro}$:LUC*) reporter and identified mutants in which *ProDH1$_{pro}$:LUC* was no longer fully down-regulated during low ψ_w stress (*16*). One drought sensitive mutant so identified had a single amino acid change in the Non-Phototrophic Hypocotyl (NPH3) domain of NPH3/RPT2-Like5 (NRL5)/Naked Pins in Yucca8 (NPY8). This led to the further surprising discovery that the NPH3-domain is a plant-specific type of GTPase that interacts with trafficking-related proteins to form a previously unknown layer of regulation relevant to protein targeting and cellular polarity.

An NPH3-domain mutation (NRL5^{P335L}) causes drought hypersensitivity because of mis-regulated proline metabolism.

Mutant number 4090 did not fully down-regulate *ProDH1$_{pro}$:LUC* expression during low ψ_w stress (Fig S1A and B), hyperaccumulated proline (Fig. S1C), was dramatically sensitive to even moderate severity (-0.7 MPa) low ψ_w which slowed, but did not stop, growth of wild type in both agar plate assays (Fig. 1A and B) and in partial soil drying (Fig. S2A and B). We identified a single amino acid substitution (P335L) in Non-Phototrophic Hypocotyl3/Root Phototropism2-Like 5 (NRL5; also known as Naked Pins in Yucca 8, NPY8) as the putative causal mutation in 4090 (hereafter referred to as *nrl5-1*, fig. S1D and E). This was confirmed by the ability of a genomic fragment containing the *NRL5* promoter and gene body (*NRL5$_{pro}$:NRL5-YFP*) to complement both *nrl5-1* (Fig. S1A and B) and a T-DNA knockdown allele (*nrl5-2;* Fig. 1B and C, fig. S1F-H, fig. S2C). In contrast, *NRL5$_{pro}$:NRL5^{P335L}-YFP* failed to complement *nrl5-2* (Fig. 1B and C, fig. S2C) despite being

expressed at similar level (Fig. S1G). *nrl5-2* also had increased DNA damage at low ψ_w (Fig. S3) and increased expression of drought-regulated genes (Fig. S4A) indicating that *nrl5* mutants were damaged by moderate severity low ψ_w which caused minimal damage to wild type.

During low ψ_w stress, *nrl5* mutants had increased transcript and protein levels of P5C synthetase1 (P5CS1), the enzyme responsible for the majority of stress-induced proline synthesis, and increased expression of *P5CS2* (Fig. S4B and fig. S5A to C), consistent with its higher level of proline accumulation. Interestingly, *nrl5-2* also had increased ProDH enzymatic activity (Fig. 1D), even though ProDH1 protein levels were not altered in *nrl5* mutants (Fig. S5B, D). Generation of double mutants between *nrl5-2* and the proline metabolism mutants *p5cs1-4*, *prodh1-2* and *p5cdh* (the latter of which lacks P5C Dehydrogenase, the enzyme which converts P5C to glutamate in mitochondria) showed that blocking proline catabolism upstream of P5C production (*nrl5-2prodh1-2*) alleviated the low ψ_w sensitivity and slower recovery of *nrl5-2* (Fig. 1E and F, fig. S6A). In contrast, blocking proline catabolism downstream of P5C production (*nrl5-2p5cdh-2, nrl5-2p5cdh-3*) did not. Partially blocking proline synthesis using *p5cs1-4* was also not sufficient to reverse the *nrl5-2* phenotype (Fig. 1E and F, fig. S6A).

In this set of mutants, low ψ_w sensitivity did not correlate with the level of low ψ_w-induced proline accumulation (Fig. S6B) but was corelated with high level of P5C (Fig. S6C) and ROS (Fig. S7). P5C and ROS were high in *nrl5-2*, *nrl5-2p5cs1-4* and *nrl5-2p5cdh* mutants but reduced to wild type level in *nrl5-2prodh1-2,* consistent with its nearly wild type level of growth in the low ψ_w and recovery treatments. Thus, *nrl5* mutants were hypersensitive to low ψ_w because of an inability to properly restrain proline catabolism and

thereby limit P5C and ROS production, despite accumulating high levels of proline which would often be associated with increased drought resistance (*2*).

NRL5, but not NRL5^{P335L}, interacts with RABH1B/RABE1C and VAMP721/722

The NRL5^{P335L} substitution is in its NPH3 domain, a plant specific protein domain of unknown function (*17*). To understand why NRL5^{P335L} had such a dramatic effect on drought resistance, we immunoprecipitated NRL5-YFP and identified RAB small GTPases and VAMP721 as putative NRL5 interactors (Data S1). GST-pull down assays demonstrated that NRL5 interacted with RABE1C and RABH1B in the presence of GTPγS, a nonhydrolyzable GTP analog which keeps RABs in their active state, but had reduced interaction in the presence of GDP (Fig. 2A; input shown in Fig. S8A). In contrast, NRL5^{P335L} did not interact with RABH1B or RABE1C even with GTPγS (Fig. 2A). We did not detect NRL5 interaction with RABA4A (Fig. S8B), indicating specificity of NRL5 interaction with certain RAB subgroups. Interestingly, the NRL5-RABE1C interaction required both proteins to be exposed to GTPγS (Fig. S8C). If only NRL5 or RABE1C, but not the other, was exposed to GTPγS, then their interaction was abolished or greatly reduced. These results suggest that GTPγS converts NRL5 to a state competent for RAB interaction.

NRL5, but not NRL5^{P335L}, interacted with VAMP721 (Fig. 2B; input Fig. S8D) and VAMP722 (Fig. S8E). This indicated that the NPH3 domain is also required for NRL5-VAMP interaction, even though this interaction did not require GTPγS. NRL5 interacted with both the Longin and SNARE domains of VAMP721, although, a more extensive interaction was observed for the Longin domain (Fig. 2B). In contrast to the RAB and VAMP interactions, NRL5 self-interaction (likely dimerization), which occurs via the BTB domain, was not blocked by the P335L mutation (Fig. 2B and fig S8F).

Ratiometric Bi-molecular fluorescence complementation (rBiFC) assays detected NRL5 interaction with both wild type and constitutively active (RABH1B^{Q68L} and RABE1C^{Q74L}) versions of RABH1B and RABE1C; but, not with constitutively inactive RABH1B^{T23N} or RABE1C^{S29N} (Fig. 2C, representative images shown in fig S9). In contrast, no interaction was detected for NRL5^{P335L} with either wild type or the constitutive active version of either RAB. Likewise, VAMP721 interacted with NRL5, but not NRL5^{P335L} (Fig. 2D and fig. S9). The rBiFC assays also confirmed that self-interaction of NRL5 was not affected by the P335L substitution (Fig. 2E and Fig. S9A). For all detectable interactions, the rBiFC signal was observed as foci close to the periphery of the cell (Fig. 2F and fig. S9B). Given the well-known functions of RABs and VAMPs in vesicle trafficking, this pattern suggested that the NRL5 interactions occurred on, or close to, vesicles. We also noted that, NRL5 self-interaction was significantly decreased by low ψ_w while NRL5 interaction with RABs and VAMP721 was increased or unchanged (Fig. 2C-E).

NRL5 GTPase activity

In the course of testing whether NRL5 influences RAB GTPase activity, we made the surprising discovery that NRL5 is itself a GTPase. P_i release catalyzed by NRL5 had a similar rate and half-maximal GTP concentration as the GTPase activity of RABH1B, RABE1C or RABA4A (Fig. 3A and fig. S10A and B). In contrast, NRL5^{P335L} had greatly reduced GTPase activity. No activity was observed when ATP, GDP or GTPγS were used as substrates (Fig. 3A). NPH3 itself, the best characterized NPH3-domain protein, had similar GTPase activity (Fig. S10A and B), indicating that other NPH3-domain proteins are also GTPases.

Use of a desthiobiotin-GTP probe, which biotinylates GTP-binding proteins (*18*), confirmed that NRL5 had GTP association (Fig. 3B). This GTP-association was greatly

impaired, but not eliminated, for NRL5^{P335L} and required Mg^{2+} as a cofactor (Fig. 3B and fig. S10C), similar to other GTP-binding proteins. LC-MS analysis of biotinylated NRL5 peptides found that desthiobiotin-GTP labeled several lysine residues flanking the P335 site critical for GTPase activity and close to conserved regions of the NPH3 domain (Fig. S11, Data S2), albeit that there was also seemingly non-specific labeling of the unstructured C-terminus and the N-terminal portion of the BTB domain which is not required for GTPase activity (see below). Sequence alignment and structural prediction showed that P335 is not conserved among NPH3-domain proteins and is thus unlikely to participate directly in GTP binding or hydrolysis. Rather it is in a linker region between conserved helices that are arranged in strikingly planar form (Fig. S11C and D). Thus, the P335L mutation could affect the spatial arrangement of the conserved helices. This could explain how NRL5^{P335L} is impaired in GTPase activity and desthiobiotin-GTP labeling, as well as in VAMP interaction which does not require GTP.

NRL5 and RABH1B/RABE1C determine each other's *in vitro* GTPase activity in a manner that can be modulated by VAMP721/722.

The switching of RAB GTPases between their active, GTP-bound state, which functions in vesicle trafficking, versus their inactive, GDP-bound, form is controlled by effector proteins (*19*). Thus, we tested whether NRL5 also acted as such an effector. Strikingly, NRL5 interaction with RABH1B or RABE1C resulted in nearly complete inhibition of GTPase activity indicating that the proteins inhibit each other's activity (Fig. 3C, left side). Truncated NRL5 lacking the BTB domain had similar ability to inhibit P_i release; however, NRL5^{P335L} failed to inhibit RABH1B or RABE1C GTPase activity (Fig. 3C). Combining NRL5 with RABA4a did not lead to the same inhibition of GTPase activity (Fig. S10D), indicating that inhibition of GTPase activity required a specific NRL5-RAB interaction. VAMP721 and VAMP722 did not affect RABH1B/RABE1C or NRL5 GTPase

activity; however, addition of VAMP721/722 to RAB-NRL5 mixtures could restore GTPase activity (Fig. 3C, right side). Thus, the dynamic between NRL5 interaction with certain RABs versus interaction with VAMP721/722 could control the activation state of RABs, and possibly NRL5 itself.

***nrl5-2* low ψ_w sensitivity requires VAMP721/722 and RABE1C.**

Given this cross-regulation of GTPase activity among NRL5 and its interaction partners, we also tested their genetic interaction in low ψ_w resistance. Most strikingly, *nrl5-2vamp721* and *nrl5-2vamp722* reverted the low ψ_w sensitivity phenotype of *nrl5-2* (Fig. 4A and B, fig. S12). Likewise, *nrl5-2rabe1c* was phenotypically similar to the *rabe1c* single mutant. These results indicated that *nrl5-2* low ψ_w hypersensitivity was caused by improper function of VAMP721/722, and RABE1C during low ψ_w stress. The *nrl5-2rabh1b* results were less clear-cut as *rabh1b* had constitutively reduced growth (Fig. 4A and B, fig. S12), consistent with report that RABH1B is involved in trafficking cellulose synthase to the plasma membrane and that *rabh1b* has cell wall defects with limit its growth (*20*).

Both RABH1B and RABE1C are involved in exocytosis and trafficking of proteins to the plasma membrane (*21, 22*). Along with VAMP721/722 function in vesicle targeting and excretion at the plasma membrane (*23-25*), the NRL5 physical and genetic interactions we observed suggest that it also is involved in trafficking to the plasma membrane. Consistent with this hypothesis, proteomic analysis found that *nrl5-2* lacked stress-induced accumulation of plasma membrane and cell wall-associated proteins and, conversely, hyperaccumulated cruciferin and seed storage proteins, which also may depend on NRL5-related trafficking to control their abundance and localization (Fig. S5A, E and F, Data S3-S5). Note also that the proteomics analysis provided no indication that *nrl5-2* had increased levels of RABH, RABE

or VAMP721/722 proteins as might be expected if NRL5 used its BTB domain to function as a ubiquitin E3 ligase to target these proteins for degradation (Fig. S5G).

A functional NPH3 domain is required for NRL5 polarization and plasma membrane localization.

NRL5 was polarly localized at the bottom of root and hypocotyl cells and was asymmetrically distributed around leaf pavement cells (Fig. 4C and fig. S13). The P335L mutation disrupted this polar localization. This could be dramatically observed in rBiFC assays of NRL5 versus NRL5^{P335L} self-interaction (Fig. S9E). Loss of polarity could also be observed in stably transformed plants (Fig. 4C and fig. S13) but was less dramatic, possibly because the formation of heterocomplexes of NRL5^{P335L} with other NRLs allowed some degree of polarity to be maintained. Low ψ_w caused a partial loss of NRL5 polarity and exacerbated the NRL5^{P335L} loss of polarity, particularly in hypocotyl and leaf pavement cells (Fig. 4C and fig. S13). This coincided with the reduction of NRL5 self-interaction during low ψ_w stress (Fig. 2E and fig. S9A). NRL5 partially co-localized with a plasma membrane marker and, similar to its polarity, this also was diminished by the P335L mutation and by low ψ_w (Fig. S14A). NRL5 did not co-localize with a plasmodesmata marker (Fig. S14B). Together, these data demonstrated that NRL5 polarity and localization, like its GTPase activity and interaction with trafficking proteins, depended upon a fully functional NPH3 domain.

Discussion

NPH3-family proteins have been implicated in key cellular processes, most notably phototropism and auxin signaling (*17, 26, 27*). However, molecular function of the NPH3 domain has remained unknown. Our results show that the NPH3-domain is a plant-specific type of GTPase. Most GTPases are involved in intracellular trafficking (*19, 28*). This, along

with NRL5 interaction with RABH1B/RABE1C and VAMP721/722, as well as their cross-regulation of each other's activities, indicate that NRL5, and other NPH3 domain proteins, have previously unrecognized functions in intracellular trafficking (Fig. S15). The high degree of NPH3-domain conservation across the more than thirty NPH3 family members in Arabidopsis indicates that GTPase activity and trafficking function is a core feature of this protein family. NRL5 is part of the NPY subgroup of NPH3-domain proteins, of which NPY1-5 are polarly localized and involved in maintaining polarity of PIN auxin transporters (*26, 27, 29*). For NPH3, it has been noted that its localization at the plasma membrane versus undefined bodies close to plasma membrane determines its activity in phototropism (*30*). Discovery of NPH3-domain GTPase activity and interaction with trafficking proteins will allow such observations to be critically re-evaluated and put into a functional context. This new knowledge of NPH3 domain molecular function will also facilitate analysis of the vast majority of NPH3-domain proteins whose cellular and physiological function is unknown. More broadly, the finding that plants have maintained a type of GTPase not found in metazoans illustrates how plants have adapted the core conserved trafficking machinery to their unique needs.

While the GTPase activity and protein interaction results provide us with broad principles about NPH3-domain function, the dramatic low ψ_w sensitivity phenotype resulting from mutation of a single NPH3-domain protein speaks to specificity among these proteins. The interaction of NRL5 with RABH1B and RABE1C, as well as proteome analysis of *nrl5-2*, support a hypothesis whereby NRL5 has a strong effect on trafficking and abundance of proteins involved in stress signaling at the plasma membrane-cell wall interface (Fig. S15). Consistent with this, RABH1B and RABE1C have been implicated in trafficking and secretion needed to build or maintain the cell wall (*20-22*) and VAMP721/722 are well known to be involved in vesicle targeting and protein secretion. That said, we cannot rule out

other trafficking-related functions of NRL5. We also do not rule out the possibility that NRL5 uses its BTB domain to act as a ubiquitin E3 ligase adaptor to target proteins for degradation in a manner similar to NPH3 control of Phototrophin degradation (*31*). NPH3 interacts with Phototropin via its C-terminal coiled-coil domain. The unstructured C-terminal domain is not conserved among NPH3 domain proteins and, in the trafficking context, may be the basis for NRL5 specificity in affecting trafficking of stress-related proteins. This, along with the role of heterodimerization between different NPH3-domain proteins, is of interest for further investigation.

nrl5 mutants demonstrated that there is potential for damaging ROS and P5C production whenever proline accumulates. Drought-related signaling pathways, which we now know require NRL5 to function properly, suppress the damaging aspects of proline catabolism and allow proline to safely accumulate (*2*). The proline metabolism profile of *nrl5* mutants (elevated P5CS along with high ProDH activity but no increase of P5CDH), resembles the proline metabolism profile required for cell death during the hypersensitive response to pathogen infection (*10, 11, 32, 33*). Thus, it is possible that in *nrl5* the cell wall-plasma membrane interface is more susceptible to damage or has changed in such a way that the plant misinterprets the low ψ_w stimulus and mounts a hypersensitive-like response. Interestingly, *nrl5-2p5cdh* had similar, or even greater, low ψ_w hypersensitivity as *nrl5-2* but did not accumulate higher levels of P5C than *nrl5* or *p5cdh*1 single mutants. Thus, it will also be of interest to determine whether a proline-P5C cycle, which serves to amplify proline-dependent ROS production in mammalian cells (*12, 13*), also exists in plants (*33, 34*) and whether such a cycle contributes to the low ψ_w hypersensitivity of *nrl5*. Overall, identification of NRL5 as both a critical protein for drought resistance and a trafficking-associated GTPase opens new avenues to improve drought resistance and understand how plant cells coordinate intracellular trafficking.

References and Notes

1. E. S. Haswell, P. E. Verslues, The ongoing search for the molecular basis of plant osmosensing. *Journal of General Physiology* **145**, 389-394 (2015).
2. P. E. Verslues *et al.*, Burning questions for a warming and changing world: 15 unknowns in plant abiotic stress. *Plant Cell* **35**, 67-108 (2023).
3. W. Feng, H. Lindner, N. E. Robbins, II, J. R. Dinneny, Growing Out of Stress: The Role of Cell- and Organ-Scale Growth Control in Plant Water-Stress Responses. *The Plant Cell* **28**, 1769-1782 (2016).
4. S. Sharma, J. G. Villamor, P. E. Verslues, Essential Role of Tissue-Specific Proline Synthesis and Catabolism in Growth and Redox Balance at Low Water Potential. *Plant Physiology* **157**, 292-304 (2011).
5. M. E. Alvarez, A. Savoure, L. Szabados, Proline metabolism as regulatory hub. *Trends in Plant Science* **27**, 39-55 (2022).
6. P. E. Verslues, S. Sharma, Proline metabolism and its implications for plant-environment interaction., in *The Arabidopsis Book doi: 10.1199/tab.0140*. (American Society of Plant Biologists http://www.aspb.org/publications/arabidopsis/, Rockville, MD, 2010), vol. doi: 10.1199/tab.0140, chap. doi: 10.1199/tab.0140.
7. G. G. K. Oh, B. M. O'Leary, S. Signorelli, A. H. Millar, Alternative oxidase (AOX) 1a and 1d limit proline-induced oxidative stress and aid salinity recovery in Arabidopsis. *Plant Physiology* **188**, 1521-1536 (2022).
8. G. Miller, H. Stein, A. Honig, Y. Kapulnik, A. Zilberstein, Responsive modes of Medicago sativa proline dehydrogenase genes during salt stress and recovery dictate free proline accumulation. *Planta* **222**, 70-79 (2005).
9. S. Sharma, P. E. Verslues, Mechanisms independent of ABA or proline feedback have a predominant role in transcriptional regulation of proline metabolism during low water potential and stress recovery. *Plant Cell and Environment* **33**, 1838-1851 (2010).
10. N. M. Cecchini, M. I. Monteoliva, M. E. Alvarez, Proline Dehydrogenase Contributes to Pathogen Defense in Arabidopsis. *Plant Physiology* **155**, 1947-1959 (2011).
11. M. Senthil-Kumar, K. S. Mysore, Ornithine-delta-aminotransferase and proline dehydrogenase genes play a role in non-host disease resistance by regulating pyrroline-5-carboxylate metabolism-induced hypersensitive response. *Plant Cell and Environment* **35**, 1329-1343 (2012).
12. J. M. Phang, Proline Metabolism in Cell Regulation and Cancer Biology: Recent Advances and Hypotheses. *Antioxidants & Redox Signaling* **30**, 635-649 (2019).
13. J. J. Tanner, S. M. Fendt, D. F. Becker, The Proline Cycle As a Potential Cancer Therapy Target. *Biochemistry* **57**, 3433-3444 (2018).
14. M. A. Ghars *et al.*, Phospholipases C and D Modulate Proline Accumulation in Thellungiella halophila/salsuginea Differently According to the Severity of Salt or Hyperosmotic Stress. *Plant and Cell Physiology* **53**, 183-192 (2012).
15. A. S. Leprince *et al.*, Involvement of Phosphatidylinositol 3-kinase in the regulation of proline catabolism in Arabidopsis thaliana. *Frontiers in Plant Science* **5**, (2015).
16. S. Shinde, J. G. Villamor, W. D. Lin, S. Sharma, P. E. Verslues, Proline Coordination with Fatty Acid Synthesis and Redox Metabolism of Chloroplast and Mitochondria. *Plant Physiology* **172**, 1074-1088 (2016).
17. J. M. Christie, N. Suetsugu, S. Sullivan, M. Wada, Shining Light on the Function of NPH3/RPT2-Like Proteins in Phototropin Signaling. *Plant Physiology* **176**, 1015-1024 (2018).

18. R. Cai, M. Huang, Y. S. Wang, Targeted Quantitative Profiling of GTP-Binding Proteins in Cancer Cells Using Isotope-Coded GTP Probes. *Analytical Chemistry* **90**, 14339-14346 (2018).
19. E. Nielsen, The Small GTPase Superfamily in Plants: A Conserved Regulatory Module with Novel Functions. *Annual Review of Plant Biology* **71**, 247-272 (2020).
20. M. He *et al.*, Rab-H1b is essential for trafficking of cellulose synthase and for hypocotyl growth in Arabidopsis thaliana. *Journal of Integrative Plant Biology* **60**, 1051-1069 (2018).
21. F.-C. Huang *et al.*, Arabidopsis RAB8A, RAB8B and RAB8D Proteins Interact with Several RTNLB Proteins and are Involved in the Agrobacterium tumefaciens Infection Process. *Plant and Cell Physiology* **62**, 1572-1588 (2021).
22. J. R. Mayers *et al.*, SCD1 and SCD2 Form a Complex That Functions with the Exocyst and RabE1 in Exocytosis and Cytokinesis. *The Plant Cell* **29**, 2610-2625 (2017).
23. E. R. Larson *et al.*, Synergy among Exocyst and SNARE Interactions Identifies a Functional Hierarchy in Secretion during Vegetative Growth(CC-BY). *Plant Cell* **32**, 2951-2963 (2020).
24. C. Kwon *et al.*, Co-option of a default secretory pathway for plant immune responses. *Nature* **451**, 835-U810 (2008).
25. L. Zhang *et al.*, SNARE proteins VAMP721 and VAMP722 mediate the post-Golgi trafficking required for auxin-mediated development in Arabidopsis. *Plant Journal* **108**, 426-440 (2021).
26. M. Glanc *et al.*, AGC kinases and MAB4/MEL proteins maintain PIN polarity by limiting lateral diffusion in plant cells. *Current Biology* **31**, 1918-+ (2021).
27. M. Furutani *et al.*, Polar-localized NPH3-like proteins regulate polarity and endocytosis of PIN-FORMED auxin efflux carriers. *Development* **138**, 2069-2078 (2011).
28. V. Vernoud, A. C. Horton, Z. Yang, E. Nielsen, Analysis of the Small GTPase Gene Superfamily of Arabidopsis. *Plant Physiology* **131**, 1191-1208 (2003).
29. J. J. Ramalho, V. A. S. Jones, S. Mutte, D. Weijers, Pole position: How plant cells polarize along the axes. *The Plant Cell* **34**, 174-192 (2021).
30. S. Sullivan, E. Kharshiing, J. Laird, T. Sakai, J. M. Christie, Deetiolation Enhances Phototropism by Modulating NON-PHOTOTROPIC HYPOCOTYL3 Phosphorylation Status. *Plant Physiology* **180**, 1119-1131 (2019).
31. D. Roberts *et al.*, Modulation of Phototropic Responsiveness in Arabidopsis through Ubiquitination of Phototropin 1 by the CUL3-Ring E3 Ubiquitin Ligase CRL3(NPH3). *Plant Cell* **23**, 3627-3640 (2011).
32. G. Fabro, Y. S. Rizzi, M. E. Alvarez, Arabidopsis Proline Dehydrogenase Contributes to Flagellin-Mediated PAMP-Triggered Immunity by Affecting RBOHD. *Molecular Plant-Microbe Interactions* **29**, 620-628 (2016).
33. A. Qamar, K. S. Mysore, M. Senthil-Kumar, Role of proline and pyrroline-5-carboxylate metabolism in plant defense against invading pathogens. *Frontiers in Plant Science* **6**, (2015).
34. G. Miller *et al.*, Unraveling Delta(1)-Pyrroline-5-Carboxylate-Proline Cycle in Plants by Uncoupled Expression of Proline Oxidation Enzymes. *Journal of Biological Chemistry* **284**, 26482-26492 (2009).
35. R. S. Austin et al., Next-generation mapping of Arabidopsis genes. Plant Journal 67, 715-725 (2011).
36. M. M. Wong et al., Phosphoproteomics of Arabidopsis Highly ABA-Induced1 identifies AT-Hook-Like10 phosphorylation required for stress growth regulation.

Proceedings of the National Academy of Sciences of the United States of America 116, 2354-2363 (2019).
37. P. E. Verslues, M. Agarwal, S. Katiyar-Agarwal, J. H. Zhu, J. K. Zhu, Methods and concepts in quantifying resistance to drought, salt and freezing, abiotic stresses that affect plant water status. Plant Journal 45, 523-539 (2006).
38. G. B. Bhaskara, T. H. Yang, P. E. Verslues, Dynamic proline metabolism: importance and regulation in water limited environments. Frontiers in Plant Science 6, (2015).
39. P. E. Verslues, in Plant Stress Tolerance: Methods and Protocols, R. Sunkar, Ed. (2010), vol. 639, pp. 301-315.
40. G. Miller et al., Unraveling Delta(1)-Pyrroline-5-Carboxylate-Proline Cycle in Plants by Uncoupled Expression of Proline Oxidation Enzymes. Journal of Biological Chemistry 284, 26482-26492 (2009).
41. V. A. Mezl, W. E. Knox, Properties and analysis of a stable derivative of pyrroline-5-carboxylic acid for use in metabolic studies. Analytical Biochemistry 74, 430-440 (1976).
42. M. Fendrych et al., Programmed Cell Death Controlled by ANACO33/SOMBRERO Determines Root Cap Organ Size in Arabidopsis. Current Biology 24, 931-940 (2014).
43. S. Lebreton, C. Cabassa-Hourton, A. Savoure, D. Funck, G. Forlani, Appropriate Activity Assays Are Crucial for the Specific Determination of Proline Dehydrogenase and Pyrroline-5-Carboxylate Reductase Activities. Frontiers in Plant Science 11, (2020).
44. A. H. C. Huang, A. J. Cavalieri, Proline oxidase and water stress-induced proline accumulation in spinach leaves. Plant Physiology 63, 531-535 (1979).
45. P. Schertl et al., Biochemical characterization of proline dehydrogenase in Arabidopsis mitochondria. Febs Journal 281, 2794-2804 (2014).
46. R. E. Basford, F. M. Huennekens, Studies on thiols. 1. Oxidation of thiol groups by 2,6-dichlorophenol indophenol. Journal of the American Chemical Society 77, 3873-3877 (1955).
47. R. Kesari et al., Intron-mediated alternative splicing of Arabidopsis P5CS1 and its association with natural variation in proline and climate adaptation. Proceedings of the National Academy of Sciences of the United States of America 109, 9197-9202 (2012).
48. C. Grefen, M. R. Blatt, A 2in1 cloning system enables ratiometric bimolecular fluorescence complementation (rBiFC). Biotechniques 53, 311-314 (2012).
49. K. Tsuda et al., An efficient Agrobacterium-mediated transient transformation of Arabidopsis. Plant Journal 69, 713-719 (2012).
50. S. Ivanov, M. J. Harrison, A set of fluorescent protein-based markers expressed from constitutive and arbuscular mycorrhiza-inducible promoters to label organelles, membranes and cytoskeletal elements in Medicago truncatula. Plant Journal 80, 1151-1163 (2014).
51. J. Jumper et al., Highly accurate protein structure prediction with AlphaFold. Nature 596, 583-589 (2021).
52. M. Varadi et al., AlphaFold Protein Structure Database: massively expanding the structural coverage of protein-sequence space with high-accuracy models. Nucleic Acids Research 50, D439-D444 (2021).
53. F. Madeira et al., Search and sequence analysis tools services from EMBL-EBI in 2022. Nucleic acids research, gkac240 (2022).

Acknowledgments: We thank S. Shinde and S. Mukuri for assistance in the early stage of NRL5 mutant characterization and complementation crosses; A. Savouré (Sorbonne Université) for advice on ProDH activity assay; J.-Y. Huang and M.-J. Feng for assistance with confocal microscopy and image quantitation and O.-K. Teh for critical reading of the manuscript.

Funding:

Academia Sinica Investigator Award AS-IA-108-L04 (PEV)

National Science and Technology Council, Taiwan NSTC 109-2311-B001-019-MY3 (PEV)

Academia Sinica, Institute of Plant and Microbial Biology (PEV)

National Science and Technology Council, Taiwan NSTC 110-2311-B-001-043-MY2 (C-CH)

Academia Sinica Core Facility and Innovative Instrument Project AS-CFII-111-209

Author contributions:

Conceptualization: PEV

Methodology: PEV, NU-T, Y-CL, C-CH

Investigation: NU-T, X-JH, Y-CL, SKS, S-SH

Visualization: PEV, NU-T

Funding acquisition: PEV, C-CH

Project administration: PEV, S-SH, C-CH

Supervision: PEV, C-CH

Writing – original draft: PEV, NU-T, X-JH

Writing – review & editing: PEV, NU-T, X-JH, C-CH, Y-CL

Competing interests: Authors declare that they have no competing interests.

Data and materials availability: For proteomic analysis of wild type and *nrl5-2*, MS raw data and Proteome Discoverer output files have been deposited with the ProteomeXchange Consortium via the jPOST repository with the data set identifier PXD040396. (Data available for review at URL: https://repository.jpostdb.org/preview/68146114463f9c7cda5626 with the code: 9538). NRL5 protein structure was obtained from AlphaFold Protein Structure Database (AlphaFold Protein Structure Database (ebi.ac.uk). Gene and protein sequence information used in this study can be obtained from The Arabidopsis Information Resource [TAIR, TAIR - Home Page (arabidopsis.org)] using accession numbers listed in the article or supplementary material. Other data are available in the main text or the supplementary material.

Supplementary Materials

Materials and Methods

Figs. S1 to S15

References (35-53)

Data S1 to S6

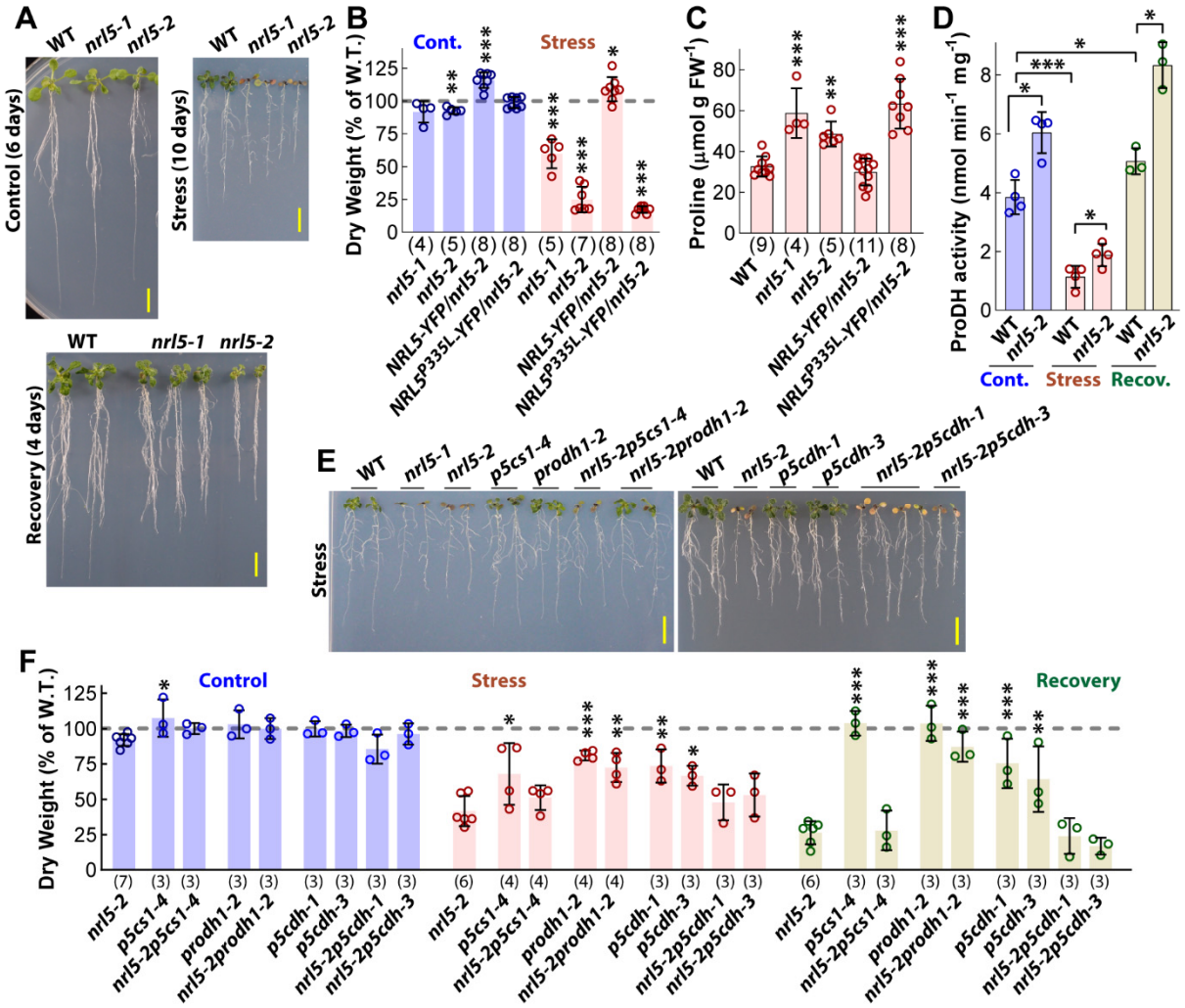

Fig. 1: *NRL5* mutants are hypersensitive to low ψ_w because of mis-regulated proline metabolism.

(**A**) *NRL5* mutants grow normally in unstressed conditions but are hypersensitive to moderate severity low ψ_w and have impaired recovery after stress release. Four-day-old seedlings were transferred to fresh control plates and imaged 5 days after transfer or transferred to low ψ_w stress (-0.7 MPa) and imaged 10 days after transfer. Stress treated seedlings were transferred back to control plates for four days for recovery. Scale bars indicate 1 cm. Images are representative from more than five independent experiments. (**B**) NRL5, but not NRL5^{P335L}, complemented *nrl5-2* low ψ_w hypersensitivity. The transgenic complementation data are combined from 3 independent transgenic lines for each construct. Data were analyzed by one sample (two-tailed) T-test comparison to wild type (WT, 100%), n values are shown in parentheses. (**C**) NRL5, but not NRL5^{P335L}, complemented the proline hyperaccumulation of *nrl5-2*. Data are from the same transgenic lines assayed in A. Data were analyzed by ANOVA comparison to WT, n values shown in parentheses. (**D**) *nrl5-2* had elevated ProDH enzymatic activity. For stress and recovery, seedlings were transferred to -0.7 MPa for 4 days and then back to control (-0.25 MPa) for one day. Data were analyzed by ANOVA, n = 4 for control and stress treatments, n = 3 for recovery. (**E**) Representative images of seedlings exposed to low ψ_w (-0.7 MPa, 10 days) show that *nrl5-2* low ψ_w sensitivity was alleviated in *nrl5-2prodh1-2* but not in double mutants with other enzymes of proline metabolism. Scale bars indicate 1 cm. Seedling images from the control and stress recovery treatments are shown in Fig. S6A. (**F**) Quantitation of seedling dry weight demonstrated that *nrl5* low ψ_w sensitivity and inability to recover growth after return to unstressed conditions was alleviated by inactivation of *ProDH1* but not *P5CS1* or *P5CDH*. Dry weight was measured five days after transfer of 5-day-old seedlings to unstressed

control (-0.25 MPa) or 10 days after transfer to low ψ_w stress (-0.7 MPa). Recovery was measured 4 days after transfer of seedlings from the stress treatment back to the high ψ_w control. Data were analyzed by ANOVA comparison to *nrl5-2* in the same treatment, n values are shown in parentheses.

For B, C, D, and F, data are from 3 or 4 independent experiments with 2 or 3 biological replicates per experiment (except D which had one replicate per experiment). Error bars show S.D. *, **, *** and N.S. indicate $P \leq 0.05$, $P \leq 0.01$, $P \leq 0.001$ and non-significant differences, respectively.

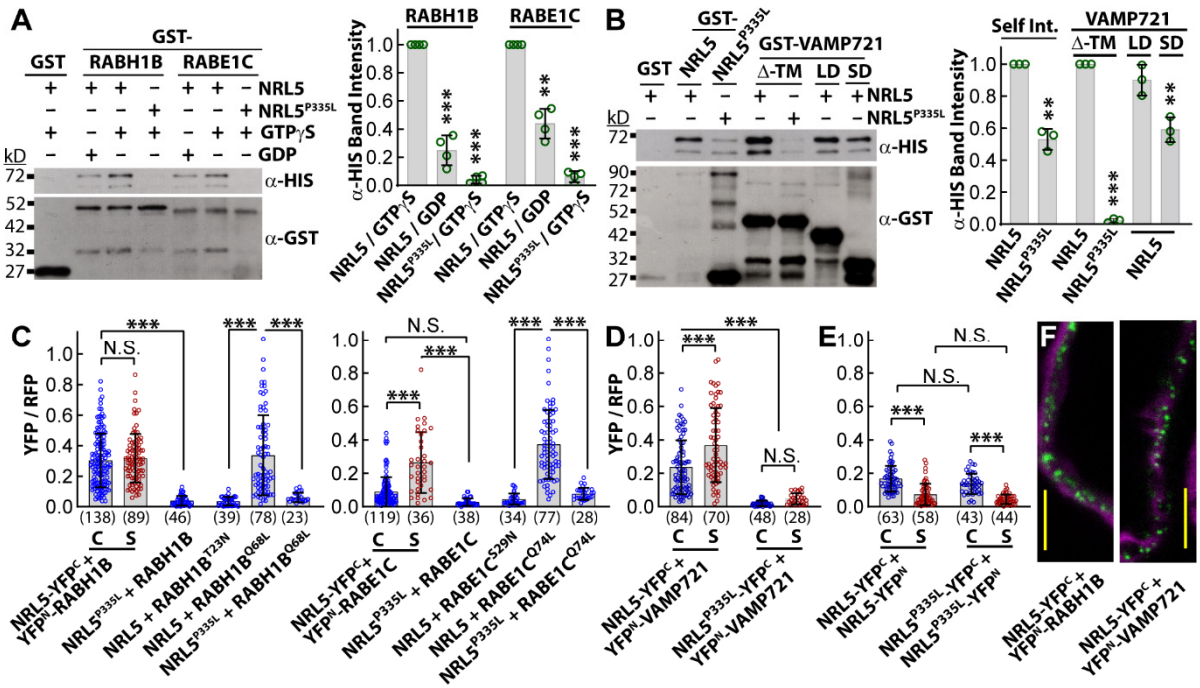

Fig. 2: NRL5 interacts with RABH1B, RABE1C and VAMP721/722.

(**A**) In vitro pull-down assay demonstrated that NRL5, but not NRL5^{P335L}, interacted with RABH1B and RABE1C in the presence of GTPγS, but had reduced interaction in the presence of GDP. Blots showing equal input of each protein are shown in Fig. S8A. Band intensity quantitative data was analyzed by one sample T-test, n = 4. (**B**) NRL5, but not NRL5^{P335L}, interacted with VAMP721 but NRL5^{P335L} could still interact with itself. Data analysis was the same as described for A but with n = 3. A similar pattern of interaction was observed for VAMP722 (Fig. S8E) and additional assays demonstrated that NRL5 self-interaction required the BTB-domain but was not substantially affect by the P335L mutation (Fig. S8F). (**C**) Quantitation of rBiFC fluorescence intensity ratio showed that NRL5 interacted with wild type or constitutively active RAB (RABH1B^{Q68L}, RABE1C^{Q74L}) but had greatly reduced interaction with inactive RAB (RABH1B^{T23N}, RABE1C^{S29N}). NRL5^{P335L} had minimal or no interaction with either wild type or constitutive active RABH1B or RABE1C. Data points are YFP/RFP ratios of individual cells and are combined from three independent experiments. Error bars indicate S.D., n values are shown in parentheses. Data were analyzed by ANOVA. C = Control, S = Stress (-0.7 MPa). (**D**) rBiFC shows interaction of NRL5 and VAMP721. The rBiFC signal was increased by low ψ_w for NRL5 but reduced to background level for NRL5^{P335L}. Data analysis and presentation are as described for C. (**E**) A similar level of rBiFC signal was detected for self-interaction of NRL5 or NRL5^{P335L} indicating that the P335L mutation does not interfere with NRL5 self-interaction. The rBiFC signal was reduced by low ψ_w treatment in both cases. (**F**) Representative rBiFC images for NRL5 interaction with RABH1B or VAMP721 in plants exposed to low ψ_w stress (Green = rBiFC signal; magenta = propidium iodide staining of cell wall). Scale bars indicate 10 μm. Additional rBiFC images can be seen in Fig. S9.

*, *** and N.S. indicate $P \leq 0.05$, $P \leq 0.001$ and non-significant differences, respectively.

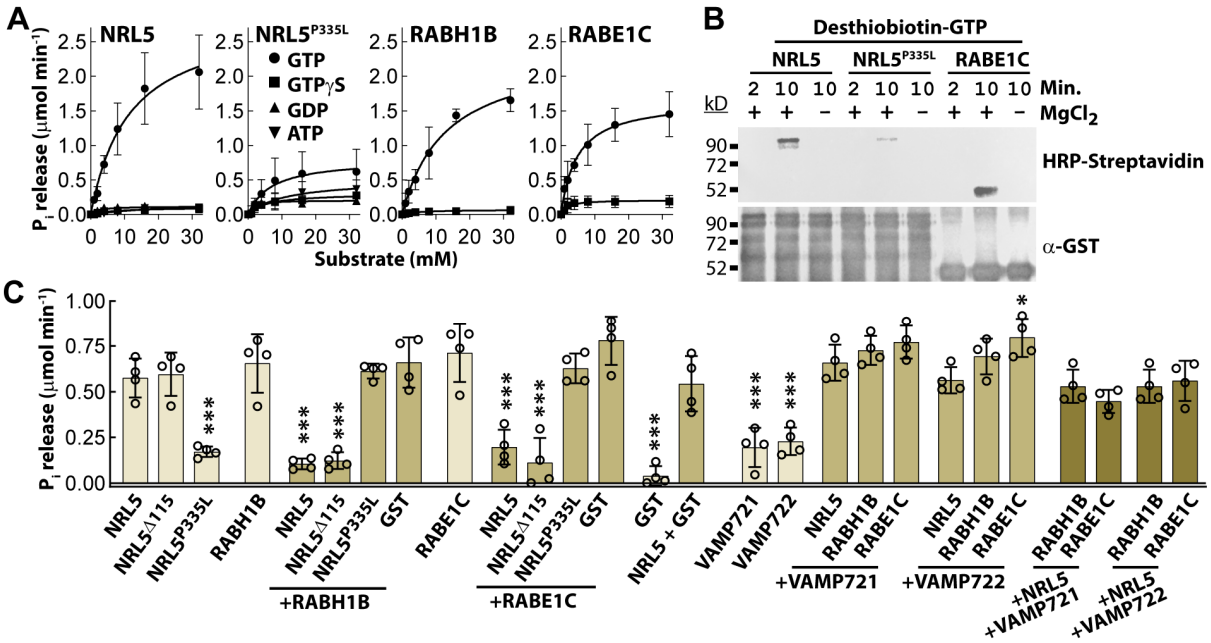

Fig. 3. NRL5 is a GTPase whose inhibition of RABH1B/RABE1C activity can be blocked by VAMP721/722.

(**A**) NRL5 had GTPase activity while activity of NRL5^{P335L} was greatly reduced. The kinetics of NRL5 GTPase activity were similar to that of RABH1B and RABE1C. One μM protein was used in each assay with the indicated substrate concentrations and P_i release quantified after 30 min. Data were analyzed by non-linear regression (K_{cat}, K_m, and V_{max} values are shown in Fig. S8A). Data are mean ± S.D. (n = 3). (**B**) Desthiobiotin-GTP labeling confirms that NRL5 associates with GTP while NRL5^{P335L} has much reduced GTP association. Proteins were incubated with Desthiobiotin-GTP for 2 or 10 minutes, or 10 minutes without $MgCl_2$. RABE1C was used as a positive control. A GST only negative control is shown in Fig. S10C. The experiment was repeated three times with consistent results. (**C**) NRL5 and RABH1B/RABE1C inhibited each other's GTPase activity while NRL5^{P335L} was unable to inhibit RAB GTPase activity. Addition of VAMP721/722 alleviated the inhibition of GTPase activity caused by NRL5-RAB interaction. Assays contained 0.25 μM of each protein and 15 mM GTP with P_i release quantified after 30 min. Data were analyzed by ANOVA comparison to NRL5 (n =4), error bars indicate S.D. Data are from one experiment out of three independent experiments conducted with consistent results. *, *** and N.S. indicate $P \leq 0.05$, $P \leq 0.001$ and non-significant differences, respectively.

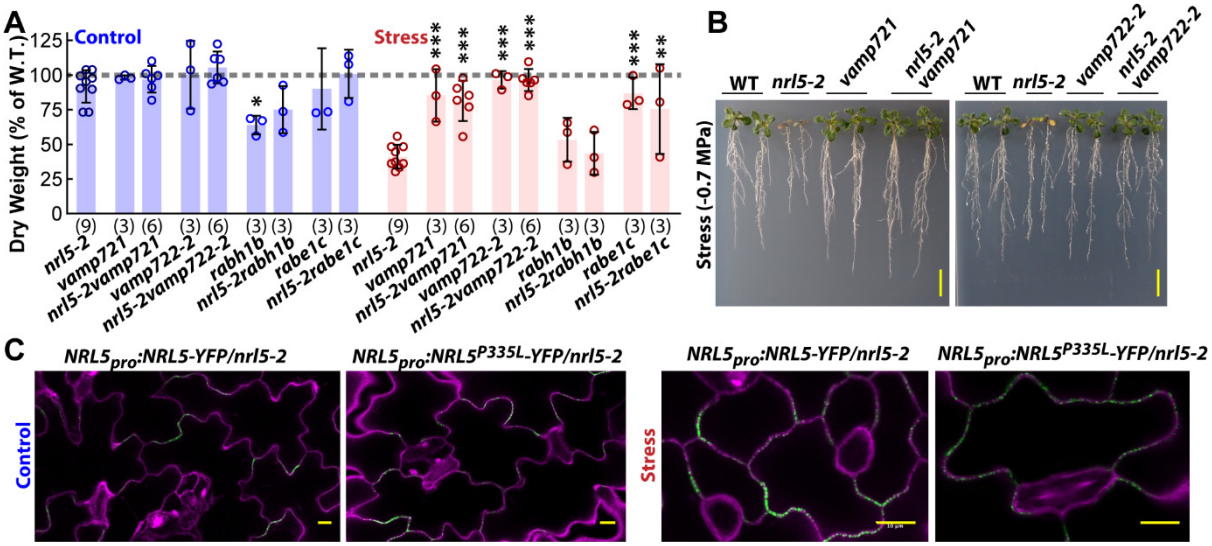

Fig 4: NRL5 polarity and genetic interaction with RABH1B, RABE1C and VAMP721/722.

(**A**) Seedling dry weight analysis shows that double mutants of *nrl5-2* with *rabe1c* or *vamp721/722* are phenotypically similar to the *rab* or *vamp* single mutants. Data are mean ± S.D. (n values indicated in parentheses, each value is from an independent experiment). Data were analyzed by ANOVA comparison to *nrl5-2* in the same treatment (n values shown in parentheses). ** and *** indicate $P \leq 0.01$ or $P \leq 0.001$, respectively. (**B**) Representative seedling images show that *nrl5-2* low ψ_w sensitivity is alleviated by mutation of *VAMP721* or *VAMP722*. Scale bars indicate 1 cm. Representative images of control seedlings and low ψ_w-treated *rab* mutants are shown in Fig. S12. (**C**) Representative images showing NRL5-YFP polarization in pavement cells and loss of polarization for $NRL5^{P335L}$-YFP. Scale bars indicate 10 µm. Additional images of NRL5 localization can be found in Fig. S13.